Detwinning in NiTi Alloys

HUSEYIN SEHITOGLU, R. HAMILTON, D. CANADINC, X.Y. ZHANG, K. GALL, I. KARAMAN, Y. CHUMLYAKOV, and H.J. MAIER

This work focuses on the stress-induced transformation in solutionized and overaged single-crystal NiTi alloys. The potential role of detwinning on the recoverable strains was investigated both theoretically and also with temperature-cycling experiments. The detwinning is the growth of one variant within a martensite in expense of the other. It is shown that the experimental recoverable strains in tension (near 8.01 pct in the [123], 9.34 pct in the [111], and 7.8 pct in the [011] orientations) exceed the theoretical martensite (correspondent-variant pair (CVP) formation strains (6.49 pct in [123], 5.9 pct in [111], and 5.41 pct in [011]), lending further support that partial detwinning of martensite has occurred in both the solutionized and overaged specimens. In compression, the experimental recoverable strains are lower than the theoretical martensite (CVP) formation strain. In the compression cases, the detwinning strain contribution is calculated to be negligible in most orientations. The transformation strains observed in overaged NiTi are similar to the solutionalized NiTi, suggesting that incoherent precipitates do not restrict the detwinning of the martensite. For the [123] orientation, it is demonstrated that the thermal hysteresis is higher in solutionized NiTi compared to the overaged NiTi. The higher thermal hysteresis can be exploited in applications involving damping and shape stability, while the lower hysteresis is suited for actuators.

I. BACKGROUND

SHAPE-MEMORY alloys have unique properties such as recoverability of deformation upon heating and pseudoelastic stress-strain behavior. The materials-science background has been documented for these alloys over the years in a variety of materials journals, but a number of issues are still under investigation, including detwinning of the martensite and the magnitude of recoverable strains. The detwinning is the growth of one variant within a martensite in expense of the other. The detwinning produces additional recoverable strain, especially in tension. It has been well known that transformation strains in NiTi alloys in tension are significantly larger than under compression. This produces differences in stress-strain response in tension *vs* compression and also in the measured transformation strains. These behaviors have been documented for textured polycrystals for some time and were documented recently for single crystals.[1,2] Further experimental results on single-crystal NiTi are needed to understand the deformation behavior when detwinning of the martensite occurs without the influence of grain boundaries. The possible role of Ti_3Ni_4 precipitates on detwinning also needs further understanding. Experimental results in this study are aimed at addressing these needs.

In previous work, we have calculated the martensite (correspondent-variant pair (CVP)) formation and CVP detwinning strains in compression[1] for selected orientations. The CVP is defined as the martensite plate with two correspondent variants. In this study, the focus is on determining both the CVP formation and detwinning strains in tension for all orientations. Transformation-strain contours are provided for both tension and compression within the stereographic triangle demonstrating orientations favorable (and also unfavorable) to detwinning. In the current work, five different crystal orientations have been selected, with [123], [111] and [011] exhibiting high degrees of detwinning in tension, [012] exhibiting moderate detwinning in tension, and [001] exhibiting no detwinning in tension.

There have been previous attempts to demonstrate the role of detwinning in the NiTi alloys, which focused on deformation in the absence of phase transformations. Van Humbeeck[3,4] and colleagues deformed NiTi at temperatures below the martensite finish temperature and observed the detwinning of the thermally induced martensite at strains of the order of 6 pct. Working with polycrystals, they showed that depending on the loading direction (rolling *vs* transverse), with respect to the type II-1 twinning (shear) direction, different degrees of detwinning develop during deformation. In the present work, the detwinning of stress-induced martensite accompanying the austenite-to-martensite transformation is of significant interest within the martensite finish temperature–to–austenite finish temperature window. The additional strain associated with detwinning can be harnessed to design microstructures with high recoverable strains. The magnitude of additional strain associated with detwinning is established as a function of crystal orientation, with both theoretical calculations and measurements.

It is well known that NiTi alloys undergo a martensitic transformation from the B2 austenitic to the B19′ martensitic phase upon cooling or upon straining. The martensite plates are internally twinned, with a predominant type II-1 twin type. Although the details of the detwinning process have not been fully understood, it is known that the detwinning influences the recoverable strains. Experimental results are

HUSEYIN SEHITOGLU, Grayce Wicall Gauthier Professor, R. HAMILTON and D. CANADINC, Graduate Assistants, and X.Y. ZHANG, Postdoctoral Associate, are with the Department of Mechanical and Industrial Engineering, University of Illinois, Urbana, IL 61801. Contact e-mail: huseyin@uiuc.edu K. GALL, Assistant Professor, is with the University of Colorado at Boulder, Boulder, CO 80309-0427.I. KARAMAN, Assistant Professor, is with Texas A&M University, College Station, TX. Y. CHUMLYAKOV, Professor, is with the Siberian Physical Technical Institute, 634050 Tomsk, Russia. H.J. MAIER, Professor, is with Lehrstuhl für Werkstoffkunde, (Materials Science), Dept. Mech. Eng. University Paderborn, 33098 Paderborn, Germany.

Manuscript submitted May 15, 2002.

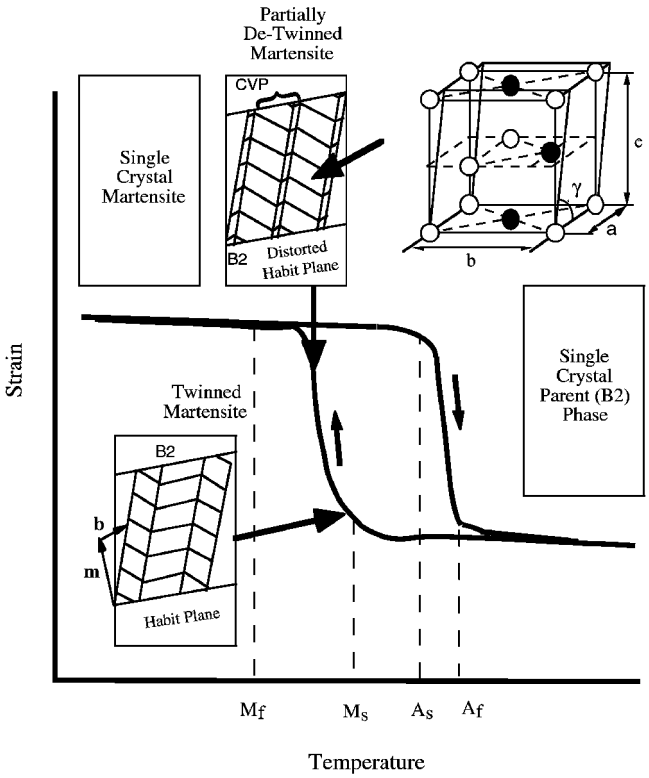

Fig. 1—Schematic of the transformation and detwinning processes during temperature cycling under tension.

presented on five crystal orientations of NiTi single crystals under temperature-cycling conditions with a constant stress. The overall recoverable strains measured exceed the CVP formation strains in tension, but not in compression. Consequently, the higher recoverable strains observed in tension are attributed to partial detwinning of the martensite.

The strain-temperature response for a single-crystal solutionized NiTi can be best described with the aid of (Figure 1). Initially, at temperatures above the austenite finish temperature ($T > A_f$) the material is in the austenitic B2 phase. A constant external stress is applied, and then the specimen is cooled to temperatures where martensite formation occurs. The transformation initiates at a critical temperature designated as the martensite start temperature. The martensite has a monoclinic crystal structure shown in the figure. The martensite that is formed is internally twinned, with two twin-related variants constituting the CVP. Upon further cooling, the martensite detwins (one twin variant grows in expense of the other), finally resulting in a single crystal of martensite. We note in Figure 1 the habit-plane normal and the shear-transformation directions. As the temperatures reach the martensite finish temperature (M_f), the martensite domains have grown throughout the entire microstructure. The presence of coherent Ti_3Ni_4 precipitates could restrict complete detwinning of the martensite, resulting in a two-phase structure with partially detwinned martensite and precipitates. If slip deformation occurs, it takes place in predominantly austenitic regions and produces a permanent (inelastic) strain. Evidence of slip deformation is provided later in this article (Section 3).

Before the experimental results are presented, we draw attention to the role of precipitates on the recoverable strains in NiTi alloys. The NiTi alloys are aged to produce nickel-rich (Ti_3Ni_4) precipitates. These precipitates can exhibit different levels of coherency and influence the transformation temperatures, the critical stress for transformation, and the slip resistance of the austenite and martensite domains. They have also been suggested to limit the detwinning process, although no experimental results have been reported. In the present work, we consider both solutionized and overaged NiTi crystals, and we show that the transformation strains for the solutionized and overaged NiTi are similar, both exceeding the CVP formation strain. The critical stresses for transformation are also comparable for both cases, with the aged case exhibiting slightly higher critical stresses.

II. THEORETICAL RESULTS—CVP FORMATION AND DETWINNING STRAINS

There are 12 independent lattice correspondences for NiTi alloys between the austenite and martensite phases.[1] The lattice parameters for the parent phase and for the monoclinic phase are $a_0 = 3.015$ Å, and $a = 2.889$ Å, $b = 4.120$ Å, $c = 4.622$ Å, and $\gamma = 96.8$ deg, respectively. The lattice correspondences are given in (Table I). These lattice correspondences allow the deformation-gradient matrix (**F**) and its symmetric part (**U**), to be determined in the cubic reference frame. There are two kinds of invariant (undistorted) planes in the twinned martensite. One is the twin plane (interface between the two lattice-correspondence variants), and the other is the habit plane. The kinematic compatibility between the two correspondence variants in the twin across the twin plane requires that[5]

$$\mathbf{R}_{ij}\mathbf{U}_j - \mathbf{U}_i = \mathbf{a} \otimes \mathbf{n} \qquad [1]$$

where $\mathbf{U}_i$ and $\mathbf{U}_j$ are two lattice-correspondence variants which form the twin, and $\mathbf{R}_{ij}$ is an orthogonal tensor (of rank 2) satisfying $\mathbf{R}_{ij}^T \cdot \mathbf{R}_{ij} = \mathbf{I}$ (**I** being the second-rank identity tensor). The $\mathbf{R}_{ij}$ term represents the relative rotation between the two variants, **n** is the twinning plane normal, **a** is the twinning shear direction. The subscripts i and j in Eq. [1] represent different choices of the integers {1, 2, . . ., 12}, and there is no summation of the index. The symbol $\otimes$ represents a dyadic product.

Using Eq. [1], all the possible twins (number of twins, twin plane normal, and twinning shear vector) can be determined. For the type II-1 case, the twin vectors are found as $\mathbf{n} = \{0.5846, 0, 0.8113\}$ and $\mathbf{a} = \langle 0.0120, 0.2890, 0.0164 \rangle$. Type II twinning has irrational twin plane normal. The type II-1 twinning is the most dominant twinning mode observed experimentally in NiTi alloys.[6] The second invariant plane condition of the habit plane is used to determine the habit-plane normal and transformation strain. The kinematic compatibility between the martensite and austenite across the habit plane requires that

$$\mathbf{F}_M - \mathbf{I} = \mathbf{b} \otimes \mathbf{m} \qquad [2]$$

where **I** is the identity tensor, **m** is the habit-plane normal, **b** is the shear of the martensite, and $\mathbf{F}_M$ is the average deformation gradient of the twinned martensite. For a stack of thin twin layers, $\mathbf{F}_M$ satisfies

$$\mathbf{F}_M = \mathbf{R}_h \left(f\,\mathbf{R}_{ij}\mathbf{U}_j + (1 - f)\mathbf{U}_i\right) \qquad [3]$$

where $\mathbf{U}_i$ and $\mathbf{U}_j$ are the two lattice-correspondence variants

Table I. The 12 Lattice Correspondence Variants*

Variant	1	2	3	4	5	6	7	8	9	10	11	12
$[100]_m$	$[100]_p$	$[\bar{1}00]_p$	$[1\underline{0}0]_p$	$[\bar{1}\underline{0}0]_p$	$[010]_p$	$[0\bar{1}0]_p$	$[01\underline{0}]_p$	$[0\bar{1}\underline{0}]_p$	$[001]_p$	$[00\bar{1}]_p$	$[\underline{0}0\bar{1}]_p$	$[\underline{0}0\bar{1}]_p$
$[010]_m$	$[0\underline{1}1]_p$	$[0\underline{1}1]_p$	$[0\underline{1}1]_p$	$[0\underline{1}1]_p$	$[10\underline{1}]_p$	$[10\underline{1}]_p$	$[10\underline{1}]_p$	$[10\underline{1}]_p$	$[\underline{1}10]_p$	$[\underline{1}10]_p$	$[\underline{1}10]_p$	$[\underline{1}10]_p$
$[001]_m$	$[011]_p$	$[011]_p$	$[011]_p$	$[011]_p$	$[101]_p$	$[101]_p$	$[101]_p$	$[101]_p$	$[110]_p$	$[110]_p$	$[110]_p$	$[110]_p$

*The *m* Refers to Martensite and *p* refers to parent (austenite).

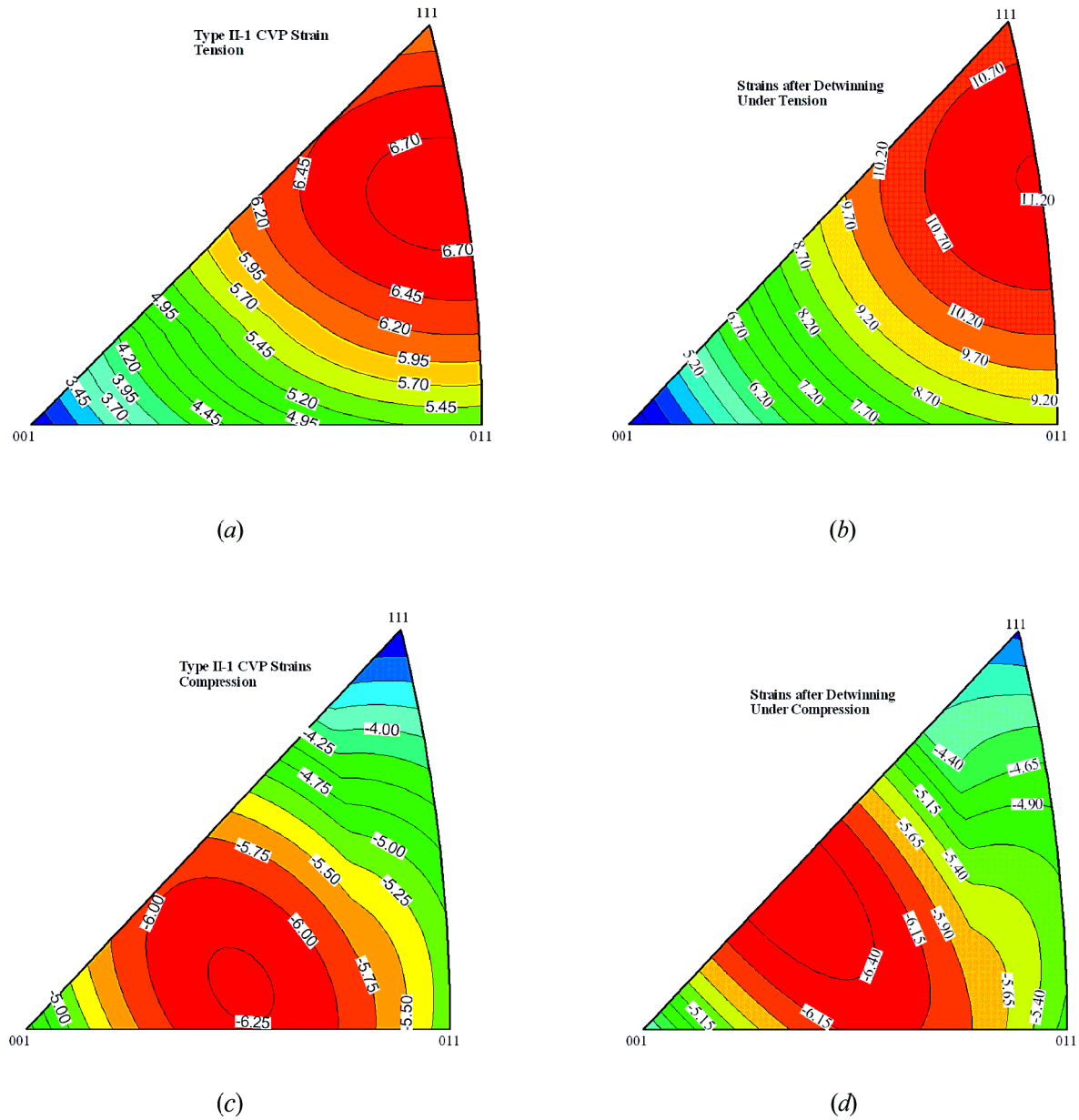

Fig. 2—Theoretical transformation strains in NiTi alloys for CVP formation and for CVP formation and detwinning: (*a*) tension CVP formation; (*b*) tension, strains after detwinning; (*c*) compression CVP formation; and (*d*) compression, strains after detwinning.

in the twin, $(1 - f)$ and f are their volume fractions, and $\mathbf{R}_h$ is the relative rotation between the twinned martensite and the parent phase. The values of $\mathbf{R}_h$ and f are unknown and are determined by solving Eq. [4] [Ref. 7].

$$\mathbf{R}_h\,(\mathbf{U}_i + f\,\mathbf{a} \otimes \mathbf{n}) = \mathbf{I} + \mathbf{b} \otimes \mathbf{m} \qquad [4]$$

There are 84 equations in Eq. [4], since there are 84 possible pairs of (**a**, **n**). The total number of habit-plane variants is 192. For the type II-1 twinning case, the **b** and **m** vectors are $\langle 0.0568, 0.0637, 0.0991\rangle$ and $\{0.8889, 0.4044, 0.2152\}$, respectively. For a type II-1 twin, it was

Table II. Summary of CVP and Detwinning Strains for the Five Crystal Orientations Studied in This Work; Both Tension and Compression Results Are Included

Type II-1	RSSF	Active CVPs	CVP Strains (Pct)	CVP + Detwinning Strain (Pct)
⟨100⟩	0.197	(5,7)(7,5)(6,8) (8,6)(9,12)(12,9) (10,11)(11,10)	2.72	2.72
⟨100⟩	−0.386	(1,3)(3,1)(1,4)(4,1) (2,3)(3,2)(2,4)(4,2)	−4.38	−4.38
⟨110⟩	0.386	(9,11)(9,12) (10,11)(10,12)	5.21	8.75
⟨110⟩	−0.430	(1,4)(4,1)(5,8)(8,5)	−5.06	−5.06
⟨111⟩	0.439	(2,3)(2,4)(6,7) (6,8)(10,11) (10,12)	5.98	10.27
⟨111⟩	−0.253	(3,1)(4,1)(7,5)(8,5) (11,9)(12,9)	−2.98	−3.58
⟨012⟩	0.355	(1,4)(2,3)	4.82	7.55
⟨012⟩	−0.508	(9,12)(12,9)	−6.23	−6.23
⟨123⟩	0.471	(2,4)	6.49	10.51
⟨123⟩	−0.464	(9,12)	−5.45	−5.53

found that there are two solutions for the volume fraction of a twin within the martensite, as $f = 0.2710$ and 0.729.

Once the habit-plane orientations and the transformation strains are determined, it is possible to establish the transformation strain as

$$\varepsilon = \frac{1}{2}(\mathbf{F}_M^T \cdot \mathbf{F}_M - \mathbf{I}) \quad [5]$$

$$= \frac{1}{2}(\mathbf{b} \otimes \mathbf{m} + \mathbf{m} \otimes \mathbf{b} + (\mathbf{b} \cdot \mathbf{b})\mathbf{m} \otimes \mathbf{m})$$

The detwinning strain (conversion of the small-volume-fraction variant to the large one within the CVP) can be determined as follows. From Eq. [3], the variant $\mathbf{U}_j$ converts to $\mathbf{U}_i$ if $f < 0.5$, and the deformation after detwinning is (by setting $f = 0$)

$$\mathbf{F}_M^{dt} = \mathbf{R}_h \mathbf{U}_i \quad [6]$$

If the volume fraction is greater than 0.5, the variant $\mathbf{U}_i$ converts to $\mathbf{U}_j$ and the transformation including detwinning is given by setting $f = 1$ (Ref. 1):

$$\mathbf{F}_M^{dt} = \mathbf{R}_h \mathbf{R}_{ij} \mathbf{U}_j = \mathbf{R}_h \cdot (\mathbf{U}_i + \mathbf{a} \otimes \mathbf{n}) \quad [7]$$

Once $\mathbf{F}_M^{dt}$ is known, the transformation strain (including CVP formation and detwinning) can be determined in a way similar to Eq. [5], with $\mathbf{F}_M$ replaced by $\mathbf{F}_M^{dt}$.

The results for CVP strains (in the absence of detwinning) and those with detwinning are presented in Figures 2(a) through (d) for all the orientations of interest. In Figures 2(a) and (b), the results are given for tension, and in Figures 2(c) and (d), the results are provided for the compression case. Two findings are noteworthy: (1) the recoverable strains in compression after detwinning are less than 60 pct of the tension results, although the maximum CVP formation strains are similar, and (2) there is considerable orientation dependence of the recoverable strain results. To gain a better understanding of the transformation strains, the theoretical results are listed in Table II for the five crystal orientations studied in this work. For the tension cases, the strains and the resolved shear stress factors (RSSFs) are indicated as positive values, while these quantities are negative for compression.

Fig. 3—TEM micrograph of NiTi overaged (823 K, 1.5 h) specimen [123] showing the precipitates and dislocations (after thermal cycling).

III. EXPERIMENTAL PROCEDURES AND DIFFERENTIAL SCANNING CALORIMETRY

The material has been obtained from Specialty Metals (New Hartford, NY). The material was nickel rich to produce precipitates upon aging with a nickel composition of 50.375 pct Ni (at. pct). The material was grown into single crystals in an inert environment using a Bridgman furnace. It was solutionized at 920 °C for 24 hours in a vacuum furnace and then quenched. A portion of the specimens were aged at 550 °C for 1.5 hours. This aging treatment produced a precipitate size near 400 nm, based on transmission electron microscopy studies (Figure 3). Figure 3 represents the thermally cycled [123] specimen, while Figure 4 demonstrates the internal twinning in the martensite. The present material has a lower volume fraction of precipitates compared to our earlier work.[1]

The experiments were conducted under thermal-cycling conditions using dog bone–type specimens. The specimens were electrodischarge machined from single-crystal ingots to have a 4 mm gage section, 2 mm width, and 1.5 mm thickness. The experiments were conducted under stress control, and a miniature extensometer was used to measure the axial deformation during the experiments. In all the experiments, the temperature was cycled between −110 °C and 80 °C. The duration of the heating and cooling was approximately 60 minutes per cycle, to minimize transient effects and thermal gradients. The heating was accomplished

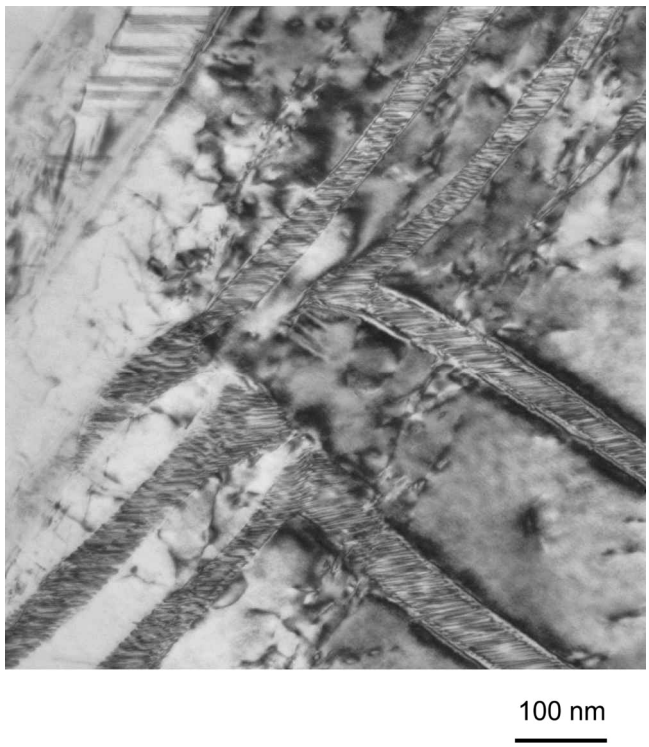

Fig. 4—TEM micrograph of NiTi overaged (823 K, 1.5 h) specimen showing the internally twinned martensite.

with induction heating. Cooling was achieved by copper tubing which surrounds the specimen and grips and is fed with liquid nitrogen.

A differential scanning calorimetry (DSC) analysis, using the Perkin–Elmer Pyris 1 machine, provided values of $A_f = 7$ °C, $A_s = -3$ °C, $M_s = -13$ °C, and $M_f = -40$ °C for the overaged NiTi. For the solutionized case, the transformation temperatures are lower and were determined to be $A_f = -20$ °C, $A_s = -48$ °C, $M_s = -35$ °C, and $M_f = -76$ °C. The DSC curves are summarized in Figure 5. These values are in qualitative agreement with the temperature-cycling results reported here, accounting for the role of stress on the transformation temperatures.

Several orientations were selected for the experiments to produce high and low levels of transformation strains in compression and tension cases. The [123], [111], and [011] orientations have high RSSFs in tension, while the [001] and [012] orientations have lower RSSFs. Based on these RSSFs, the critical stress levels for transformation and the transformation strains are expected to differ among the different orientations. In tension, the softer orientations (higher RSSF) exhibit higher transformation strains. Another difference between the orientations is that a single CVP is activated in the [123] case, while multiple CVPs are activated for the other orientations (Table II). In compression, the [111] and [011] orientations are harder, compared to the [123] and [001] cases. The [123] orientation represents high transformation strains in both tension and compression.

IV. STRAIN-TEMPERATURE RESPONSE OF SOLUTIONIZED AND OVERAGED NiTi

The strain-temperature behavior in the [123] orientation is provided in both the aged and the solutionized cases in

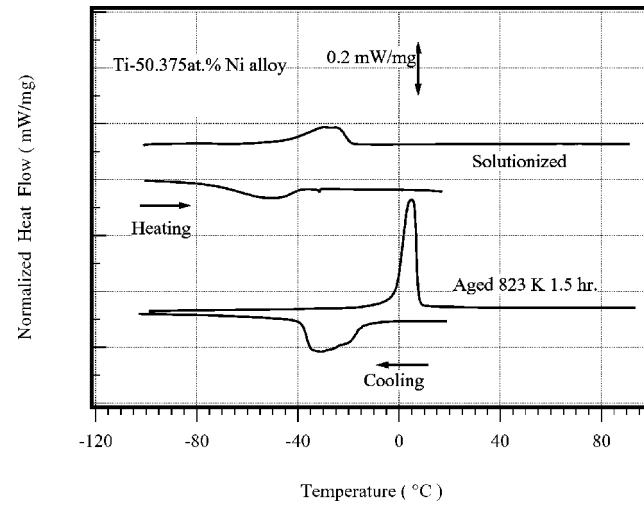

Fig. 5—DSC results on the solutionized and overaged specimens of NiTi.

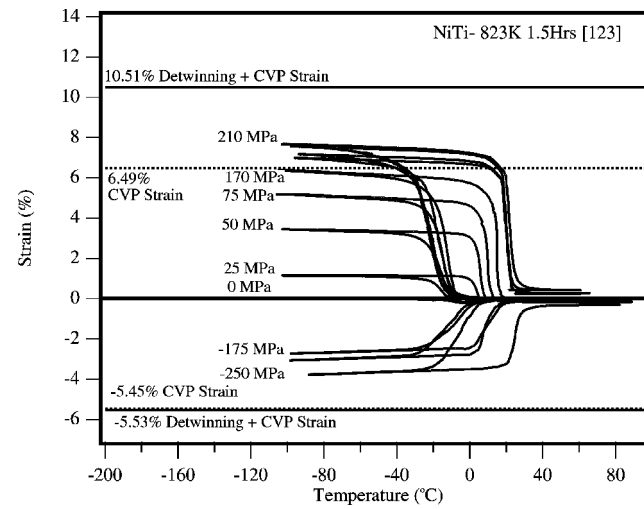

Fig. 6—Strain-temperature behavior in tension for the [123] orientation (823 K, 1.5 h).

Figures 6 and 7, respectively. The stress levels are indicated in the figures and are maintained constant in these experiments. It was found that the stress level had to be selected precisely to produce the maximum recoverable strains. Too-high levels of stress in tension induce plastic deformation and fracture, while too-low levels of stress do not produce sufficient transformation strains. A "staircase" procedure was adopted, where the stress level was gradually increased (in increments of 10 or 25 MPa) from test to test until the recoverable strains no longer increased. As much as ten to 12 stress levels were considered per condition. The stress level that produced the maximum recoverable strains is defined as the "critical stress." A similar procedure was adopted for the compression cases. In Figure 6, at 210 MPa, the maximum strain level has been reached in tension, while the critical stress level is 250 MPa in compression. It is noted that the experimental recoverable strains in tension (near 8.01 pct in the [123] orientation) exceed the theoretical martensite (CVP) formation strain (6.49 pct in the [123] orientation). The experimental strains are below the maximum theoretical strains after detwinning (10.51 pct in the

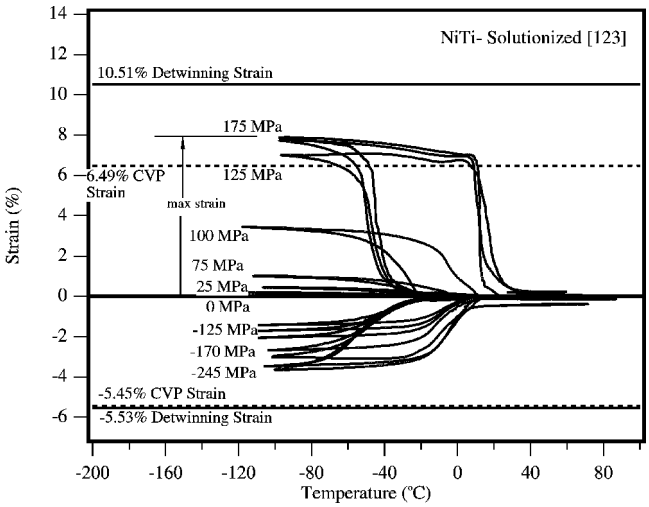

Fig. 7—Strain temperature behavior for the solutionized case, [123] orientation.

[123] case). The results for the solutionized case are shown in Figure 7. Similarly, the transformation strains exceed the CVP formation strain in the [123] solutionized tension case. These results lend further support that partial detwinning of martensite has occurred in both the solutionized and overaged specimens. In compression, the experimental recoverable strains (3.7 pct in the [123] orientation) are considerably lower than the martensite (CVP) formation strain (5.45 pct in the [123] orientation). The detwinning strain contribution is negligible in the case of compression.

It is worth noting that the thermal hysteresis (difference between the austenite finish and martensite start temperatures) is higher for the solutionized case compared to the overaged case. The maximum thermal hysteresis is 45 °C for the overaged case and 55 °C for the solutionized case, based on Figures 6 and 7. The thermal hysteresis increases slightly with increasing stress level. When compression results are examined for the [123] case, the solutionized and overaged recoverable strains are similar and the critical stress levels are −245 MPa for solutionized NiTi and −250 MPa for the overaged NiTi. For tension of [123] crystals, the critical stress levels were 210 MPa for overaged NiTi and 175 MPa for solutionized NiTi.

A summary of all the results is given in Figure 8. Each experiment is represented with a data point. The absolute value of the transformation strains is plotted for compression to portray all the results in a compact fashion. In this study, five different crystal orientations were considered in tension, with a total of 80 experiments. The theoretical detwinning strains are demonstrated by the highlighted regions. The detwinning strains are rather substantial in the [111], [123], and [011] orientations, with levels larger than 3 pct. The detwinning strain is zero in the [001] direction. In Figure 8, as the tensile stress levels increased, the transformation strains increased and then reached a plateau level. Only in the [001] case, even for stresses above 200 MPa, the transformation strains are confined to less than 2 pct.

The results in Figures 6 through 8 indicate that the recoverable strains in tension are between the CVP formation and detwinning levels. While in compression, no appreciable detwinning increment is expected, based on the observation that the experimental recoverable strains fall significantly short of the theoretical levels. The amount of detwinning in compression is rather small (less than 1 pct) compared to in tension (nearly 5 pct) in NiTi alloys, based on the theoretical results. The lack of detwinning in compression has been surmised in previous studies based on the stress-strain response,[7,8] where an extended plateau region was observed in tension and not in compression. The present results confirm the significant role of detwinning on tension-compression asymmetry in NiTi.

V. DISCUSSION OF RESULTS

The results provide significant evidence of the ability of the NiTi alloys to attain high recoverable strains (including detwinning). Transformation strains (near 9.5 pct) were obtained for the solutionized NiTi, which correspond to the combined CVP (twinned martensite) formation and partial detwinning of the CVP. It is expected that the polycrystalline forms of these alloys can limit the detwinning process due to grain boundaries. The suppression of detwinning is also expected in the presence of peak-aged precipitates with strong internal stress fields. In the case of overaged crystals, the internal stresses are relaxed, and the recoverable strains are similar to the solutionized NiTi results (Figures 6 through 8). The small difference is attributed to the inability of the precipitates to transform, hence, lowering the volume that can be transformed to martensite.

The striking similarity of the overaged and solutionized–crystal results allows us to conclude that the incoherent precipitates do not curtail detwinning in the NiTi alloys. This finding, along with our early observations that the transformation strains in incoherent precipitated NiTi are higher compared to the semicoherent precipitated NiTi,[2] opens an area of designing NiTi microstructures that are conducive to high transformation strains. It is carefully noted that the transformation strains reported in the present work can exceed the levels obtained under isothermal loadings in tension, but not in compression (Figure 8). To realize higher transformation strains in compression, the stress level needs to be raised (as opposed to maintaining it constant) to activate successive variants.

The maximum transformation strains corresponded to a critical stress level which was established systematically in this study. This critical stress level for the [123] tension overaged case was 210 MPa. In the present work, the strain-temperature response for the first cycle is demonstrated. When cycling continues beyond the first cycle, two possibilities exist. At stress levels below the critical stress, the strain-temperature curve is stable and the second cycle is a repeat of the first, and so on. When the tensile stress level is raised above the critical stress, progressive inelastic deformation occurs. Consequently, the overall strains do not increase with further increases in stress.

The present results clearly show that detwinning strains make a considerable contribution to the recoverable strain of NiTi shape-memory alloys. Micromechanical models, which attempt to predict the stress-strain behavior and recovery of NiTi (either under shape memory or pseudoleasticity), must, therefore, account for detwinning strains in addition to the martensite formation strains. Most models typically only account for the martensite formation strains, although the role of detwinning is becoming more recognized.[2,7,8] For

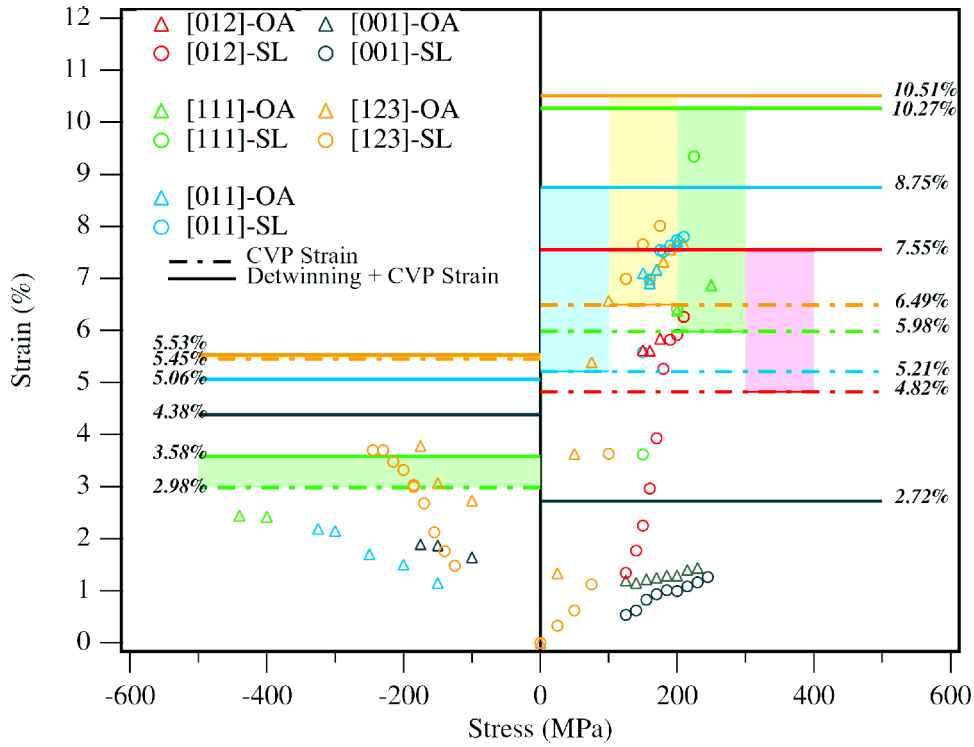

Fig. 8—Summary of temperature cycling experiments in tension and compression under stress for all orientations studied. The shaded areas indicate, detwinning contributions (OA-823 K 1.5 hr, SL-solutionized).

example, if detwinning is neglected, the tension-compression asymmetry commonly observed in experiments cannot be fully captured.

Overall, the results presented in this work are far from the idealized strain-temperature material response that has been discussed in the theoretical treatments.[10,11] Some of the experimental observations include (1) gradual rather than abrupt variations in strain at the transformation temperatures, especially during the cooling portions of the curves, (2) the wider hysteresis in the case of the solutionized *vs* the overaged case, and (3) the strong stress dependence of the transformation temperatures for the cooling portions of the curves, along with a lack of stress dependence for the heating portion of the curves. Patoor[10] and, later, Gall and Sehitoglu[11] used an interaction matrix to reflect the role of variant-variant interaction on strain hardening in NiTi loadings. These models will predict a more gradual transformation upon cooling (a nonlinear strain-temperature response rather than an abrupt transitions). But, no comprehensive model exists that can mimic the complex experimental trends observed in the present work. The narrower hysteresis is expected in the presence of internal stresses due to slipped domains. It is surmised that the slipped domains are more pronounced in the overaged than in the solutionized case.

The present experiments are in qualitative agreement with the work of Miyazaki *et al.*[9] under shape-memory conditions. In the early experiments of Miyazaki[9] (focusing on tensile loadings) and the authors,[7,8] deformation occurred at constant temperature and the shape-memory strains were measured upon heating to greater than austenite finish temperatures at zero load. In this study, a constant stress is imposed. The present results have the advantage that they intuitively provide a clearer picture of the transformation temperatures and their variations with systematic increases in stress level. In NiTi alloys, the localized slip in austenitic domains, particularly near the precipitates, have been reported to prevent high levels of transformation strains. In the present experiments, as the stress level is gradually ramped from one experiment to the next, and at high stress levels, inelastic deformation occurs and limits the transformation strain. The transmission electron microscope results shown in Figure 3 confirm the presence of slip activity in the [123] crystals.

The orientation dependence of the transformation temperatures (under stress) is a result of the relative positions of the crystal orientations on the stereographic triangle. The shift in the martensite start temperature in transforming alloys obey the Clausius–Clapeyron equation in the form

$$\frac{d\sigma}{dT} \approx \frac{\Delta H}{T\varepsilon_0} \qquad [8]$$

In the previous equation, ε_0 is the transformation strain (which is orientation dependent), ΔH is the enthalpy of the transformation, and T is the equilibrium temperature. This equation predicts that the phase boundary between the parent phase and the martensite is a function of stress, which is consistent with experimental observations. It is observed that the transformation temperatures in compression are higher by nearly 25 °C compared to those in tension. This observation is consistent with the higher $d\sigma/dT$ values (due to lower ε_0 levels) in compression relative to tension. A relative shift in the martensite start temperature (nearly 20

°C) occurs with stress for the tension-solutionized case when the stress is raised from 150 to 175 MPa. Similar shifts have been observed in compression, however, with extended tails in the strain-temperature curves. The increase of transformation temperatures with the introduction of aging is related to the lowering of Ni content in solution, as observed in previous studies.[12] A decrease in the Ni concentration has been known to raise M_s.[12] Thus, a change in the nominal composition of the matrix (the only material which undergoes the martensitic transformation) will affect the transformation if the Ni loss is significant.

For the cases considered, the area under the strain-temperature curve (hysteresis) is not constant for different orientations, stress states (tension and compression), or the two heat treatments. The higher transformation-strain orientations produce higher hysteresis levels. The crystallographic texture will be important for polycrystalline versions of these alloys, as they are often used in drawn form. Depending on the application, a large or a small thermal hysteresis is desirable. For sensor-actuator applications, a large shape change corresponding to a small change in temperature or an electric signal is needed. In pipe-coupling applications, a higher thermal hysteresis ensures the stability of the joint to small variations in temperature. Also, in coil springs or applications where maximum damping is needed, solutionized NiTi could produce better results than overaged NiTi.

The results also explain why it is more difficult to obtain a pseudoelastic response for the case of solutionized materials.[12] The criteria for pseudoelasticity, according to Liu and Galvin,[13] is written as

$$\sigma_y > 2\sigma_0 + (A_f - M_s)\frac{d\sigma}{dT} \qquad [9]$$

where $A_f - M_s$ is the thermal hysteresis, σ_0 is the minimum stress level required for stress-induced martensitic transformation, σ_y is the austenite yield strength, and $d\sigma/dT$ is the slope of the transformation stress-temperature curve. We can assume that the minimum stress levels and $d\sigma/dT$ are comparable for the solutionized and overaged cases. However, the thermal hysteresis for the solutionized case is nearly 25 °C higher than for the overaged case (Figures 6 and 7). Based on the pseudoleasticity criteria given as Eq. [9], it can be shown that the austenite strength needs to exceed 580 MPa (using $A_f - M_s = 60$ °C, $d\sigma/dT = 8$ MPa/°C, and $\sigma_0 = 100$ MPa[1]) for pseudoelasticity. For the nickel-rich NiTi compositions,[14] this condition is readily met for the solutionized condition leading to a pseudoelastic response at low temperatures.

The theoretical treatment presented here, namely, the combined CVP formation and detwinning strain determination, conforms to the transformation-strain calculations of Saburi and Nenno[15] based on lattice-correspondence variants. The exact values of transformation strains, the rotation tensor, and the crystal-orientation dependence differ between the two approaches.[2] In our calculations, for a given orientation, we have determined the detwinning of the most-favorably-oriented CVP to determine the overall transformation strains. The transformation-strain results would be different if the formation of the most-favorably-oriented single crystal of martensite was considered in a single step.

VI. CONCLUSIONS

1. Theoretical transformation strains encompassing contributions from martensite formation and detwinning are documented for numerous crystal orientations. It is shown that the role of detwinning under compression is rather small (less than 1 pct), but is very significant for tension loadings (as high as 5 pct). The detwinning is crystal-orientation-dependent and is highest near the [111] and [011] poles of the stereographic triangle.
2. The experimental transformation-strain levels in tension consistently exceeded the martensite formation strain for the [123], [111], [011], and [012] crystal orientations. These results confirm that partial detwinning of the martensite contributes significantly to the overall recoverable strains. The transformation strains in compression fall short of the theoretical levels in both crystal orientations.
3. The results confirm that the solutionized NiTi exhibits slightly higher transformation strains compared to the overaged NiTi. This small difference is attributed to the presence of Ti_3Ni_4 precipitates lowering the volume available for transformation. It is noted that the solutionized NiTi exhibits lower transformation temperatures compared to overaged NiTi. The shift in transformation temperatures is explained based on the compositional changes in the matrix.
4. Higher levels of applied stress under temperature cycling produce higher recoverable strains, but the effect saturates once a critical stress level is reached. For the soft orientations in tension, the strain levels reach their maximum values as the stresses reach 200 MPa. However, for compression, the stress levels were higher than 300 MPa to achieve the highest strains.

ACKNOWLEDGMENTS

Portions of the research are supported by a grant from the National Science Foundation, Contract No. CMS 99-00090, Mechanics and Materials Program (Arlington, VA), and Air Force Office of Scientific Research, Directorate of Aerospace and Materials Sciences (Arlington, VA). Professor Chumlyakov received support from the Russian Fund for Basic Researches, Grant Nos. 02-95-00350 and 99-03-32579.

REFERENCES

1. H. Sehitoglu, I. Karaman, R. Anderson, X. Zhang, K. Gall, H.J. Maier, and Y. Chumlyakov: *Acta Mater.*, 2000, vol. 48 (13), pp. 3311-26; 2001, vol. 49 (4), p. 747.
2. K. Gall, H. Sehitoglu, Y. Chumlyakov, and I. Kireeva: *Acta Mater.*, 1999, vol. 47 (4), pp. 1203-17.
3. Z. Xie, Y. Liu, and J. Van Humbeeck: *Acta Mater.*, 1998, vol. 46 (6), pp. 1989-2000.
4. Y. Liu, Z.L. Xie, J. Van Humbeeck, and L. Dealey: *Acta Mater.*, 1999, vol. 47 (2), pp. 645-60.
5. J.M. Ball and R.D. James: *Arch. Rat. Mech. Anal.*, 1987, vol. 100, pp. 13-52.
6. M.H. Nishida, H. Ohgi, I. Itai, A. Chiba, and K. Yamauchi: *Acta Mater.*, 1995, vol. 43, pp. 1219-27.
7. K. Gall, H. Sehitoglu, R. Anderson, I. Karaman, Y.I. Chumlyakov, and I.V. Kireeva: *Mater. Sci. Eng. A*, 2001, vol. 317 (1–2) pp. 85-92.
8. H. Sehitoglu, R. Anderson, I. Karaman, K. Gall, and Y. Chumlyakov: *Mater. Sci. Eng. A*, 2001, vol. 314 (1–2), pp. 67-74.

9. S. Miyazaki, S. Kimura, K. Otsuka, and Y. Suzuki: *Scripta Mater.*, 1984, vol. 18, pp. 883-88.
10. E. Patoor, M. El Amrani, A. Eberhardt, and M. Berveiller: *J. Phys.*, 1995, vol. 5, pp. C2-495-C2-500.
11. K. Gall and H. Sehitoglu: *Int. J. Plasticity*, 1999, vol. 15, p. 69.
12. K. Gall, H. Sehitoglu, Y.I. Chumlyakov, I.V. Kireeva, and H.J. Maier: *ASME, JEMT*, 1999, vol. 121, pp. 19-27; vol. 121, pp. 28-37.
13. Y. Liu and S.P. Galvin: *Acta Mater.*, 1997, vol. 45 (11), pp. 4431-39.
14. H. Sehitoglu, J. Jun, X. Zhang, I. Karaman, Y. Chumlyakov, H.J. Maier, and K. Gall: *Acta Mater.*, 2001, vol. 49 (17), pp. 3609-20.
15. I. Saburi and S. Nenno: *Proc. Int. of Solid-Solid Phase Transf.*, Pittsburgh, 1981, pp. 1455-79.